

The O2-independent pathway of ubiquinone biosynthesis is essential for denitrification in Pseudomonas aeruginosa

Chau-Duy-Tam Vo, Julie Michaud, Sylvie Elsen, Bruno Faivre, Emmanuelle Bouveret, Frédéric Barras, Marc Fontecave, Fabien Pierrel, Murielle Lombard, Ludovic Pelosi

▶ **To cite this version:**

Chau-Duy-Tam Vo, Julie Michaud, Sylvie Elsen, Bruno Faivre, Emmanuelle Bouveret, et al.. The O2-independent pathway of ubiquinone biosynthesis is essential for denitrification in Pseudomonas aeruginosa. Journal of Biological Chemistry, 2020, 295 (27), pp.9021-9032. 10.1074/jbc.RA120.013748 . pasteur-02746713

HAL Id: pasteur-02746713
https://pasteur.hal.science/pasteur-02746713

Submitted on 5 Nov 2020

HAL is a multi-disciplinary open access archive for the deposit and dissemination of scientific research documents, whether they are published or not. The documents may come from teaching and research institutions in France or abroad, or from public or private research centers.

L'archive ouverte pluridisciplinaire **HAL**, est destinée au dépôt et à la diffusion de documents scientifiques de niveau recherche, publiés ou non, émanant des établissements d'enseignement et de recherche français ou étrangers, des laboratoires publics ou privés.



Distributed under a Creative Commons Attribution - NonCommercial 4.0 International License

The O_2-independent pathway of ubiquinone biosynthesis is essential for denitrification in *Pseudomonas aeruginosa*

Chau-Duy-Tam Vo[1¶], Julie Michaud[2¶], Sylvie Elsen[3], Bruno Faivre[1], Emmanuelle Bouveret[4,5], Frédéric Barras[4,5], Marc Fontecave[1], Fabien Pierrel[2], Murielle Lombard[1]* and Ludovic Pelosi[2]*

[1]Laboratoire de Chimie des Processus Biologiques, Collège de France, CNRS UMR 8229, PSL Research University, Sorbonne Université, Paris, France ; [2]CNRS, CHU Grenoble Alpes, Grenoble INP, TIMC-IMAG, Université Grenoble Alpes, Grenoble, France; [3]Biology of Cancer and Infection, U1036 INSERM, CEA, Université Grenoble Alpes, ERL5261 CNRS, Grenoble, France; [4]SAMe Unit, Department of Microbiology, Institut Pasteur, Paris, France; [5]IMM-UMR 2001 CNRS-Institut Pasteur, Paris, France

Running title: *Ubiquinone is essential for denitrification in Pseudomonas aeruginosa*

*To whom correspondence should be addressed: ludovic.pelosi@univ-grenoble-alpes.fr, murielle.lombard@college-de-france.fr

¶ C.-D.-T.V. and J.M. contributed equally to the work.

Keywords: ubiquinone biosynthesis, coenzyme Q, anaerobic respiration, denitrification, *Pseudomonas aeruginosa*, iron-sulfur protein, UbiV, UbiU, UbiT, bacterial metabolism, hydroxylation, oxygen, quinone.

ABSTRACT

Many proteobacteria, such as *Escherichia coli*, contain two main types of quinones, benzoquinones represented by ubiquinone (UQ) and naphthoquinones such as menaquinone (MK) and dimethyl-menaquinone (DMK). MK and DMK function predominantly in anaerobic respiratory chains, whereas UQ is the major electron carrier in the reduction of dioxygen. However, this division of labor is probably not very strict. Indeed, a pathway that produces UQ under anaerobic conditions in an UbiU-, UbiV-, and UbiT-dependent manner has been recently discovered in *E. coli*. However, its physiological relevance is not yet understood because MK and DMK are also present in *E. coli*. Here, we established that UQ_9 is the major quinone of *Pseudomonas aeruginosa* and is required for growth under anaerobic respiration (i.e. denitrification). We demonstrate that the ORFs *PA3911*, *PA3912*, and *PA3913*, which are homologs of the *E. coli ubiT*, *ubiV* and *ubiU* genes, respectively, are essential for UQ_9 biosynthesis and thus for denitrification in *P. aeruginosa*. These three genes hereafter are called $ubiT_{Pa}$, $ubiV_{Pa}$, and $ubiU_{Pa}$. We show that $UbiV_{Pa}$ accommodates an iron–sulfur [4Fe-4S] cluster. Moreover, we report that $UbiU_{Pa}$ and $UbiT_{Pa}$ can bind UQ and that the isoprenoid tail of UQ is the structural determinant required for recognition by these two Ubi proteins. Since the denitrification metabolism of *P. aeruginosa* is believed to be important for pathogenicity of this bacterium in individuals with cystic fibrosis, our results highlight that the O_2-independent UQ biosynthetic pathway may represent a possible target for antibiotics development to manage *P. aeruginosa* infections.

INTRODUCTION

The opportunistic pathogen *Pseudomonas aeruginosa* has a remarkable ability to grow under a variety of environmental conditions such as soil and water as well as animal-, human-, and plant-host-associated environments. *P. aeruginosa* is responsible for numerous acute and chronic infections and poses a major health risk for patients with severe burns, cystic fibrosis (CF) or in severely immunocompromised states (1,2).

The utilization of various carbon sources and energy metabolism (respiration or fermentation) might contributes to the environmental adaptation of *P. aeruginosa* (3). Its main energy-producing system is respiration, which requires a proton motive force (pmf) used for ATP synthesis. The pmf is produced by the transfer of electrons and protons from reduced donors to oxidized acceptors *via* the quinone pool. Whereas the

dehydrogenases and reductases involved in respiratory metabolism have been well described and annotated in the genome of *P. aeruginosa* PAO1 (4,5), the composition of its quinone pool has not yet fully established. Studies in the sixties suggested ubiquinone 9 (UQ_9) as a major quinone of aerobically-grown *P. aeruginosa* (6) and UQ_9 is therefore believed to be essential for aerobic respiration (7).

Proteobacteria contain two main types of quinones, benzoquinones and naphthoquinones, represented respectively by UQ (or coenzyme Q) and menaquinone (MK) / demethylmenaquinone (DMK) (8). Typically, MK and DMK function predominantly in anaerobic respiratory chains, whereas UQ is the major electron carriers used for reduction of dioxygen by various cytochrome oxidases (8). Recent data indicated that the metabolic use of various quinone species according to environmental dioxygen availability might be more complex than initially thought. Indeed, using *E. coli* as a model, we highlighted a pathway conserved across many bacterial species and able to produce UQ under anaerobic conditions (9). The classical UQ biosynthetic pathway requires O_2 for three hydroxylation steps (10). Obviously, the flavin-dependent monooxygenases UbiI, UbiF, and UbiH, which catalyze the O_2-dependent hydroxylation steps are not involved in the anaerobic pathway, nor are the accessory UbiK and UbiJ proteins implicated in the assembly and/or stability of the aerobic Ubi-complex (11). Seven proteins (UbiA, B, C, D, E, G and X) catalyzing the prenylation, decarboxylation and methylation of the phenyl ring of the 4-hydroxybenzoate precursor are common to both pathways (9). In addition, the anaerobic pathway requires UbiT, UbiU and UbiV proteins. UbiT is homologous to UbiJ and UbiU and UbiV are expected to be involved in O_2-independent hydroxylations (9). However, as explained above, the metabolic relevance of the O_2-independent UQ pathway is not yet clearly understood to date.

In absence of O_2, *P. aeruginosa* is able to carry out anaerobic respiration with nitrate and nitrite as terminal electron acceptors of the respiratory chain. This process called denitrification allows the reduction of soluble nitrate (NO_3^-) and nitrite (NO_2^-) to gaseous nitrous oxide (N_2O) or molecular nitrogen (N_2) (12). Because *P. aeruginosa*-infected mucus in CF airway is depleted of oxygen and enriched in nitrate and nitrite, the anaerobic metabolism of *P. aeruginosa* via the denitrification pathway is believed to be important for its pathogenicity (13). Four sequential reactions involving metalloenzymes are needed to reduce nitrate to N_2, i.e. nitrate reductase, nitrite reductase, nitric oxide reductase and nitrous oxide reductase. *P. aeruginosa* was considered as a paradigm of the denitrification pathway and all the reductases involved in this metabolism have been widely studied as well as the regulatory network controlling the denitrification genes (3,4,14). However, the anaerobic quinone pool of *P. aeruginosa* has not been characterized so far.

In the present study, we discovered that UQ_9 is essential for the growth of *P. aeruginosa* PAO1 strain in denitrification medium. We identified in this bacterium the ORFs *PA3911*, *PA3912* and *PA3913* as homologs to *E. coli ubiT*, *ubiV* and *ubiU*, respectively. Our results showed that these three genes hereafter called $ubiT_{Pa}$, $ubiV_{Pa}$ and $ubiU_{Pa}$ are essential components of the O_2-independent UQ_9 biosynthetic pathway of *P. aeruginosa*. We demonstrated that i), $UbiV_{Pa}$ binds a [4Fe-4S] cluster and ii) $UbiU_{Pa}$ and $UbiT_{Pa}$ copurify with UQ by recognizing the isoprenoid tail. Such a molecular pathway for UQ production was found only in proteobacteria (9) where it can exert an essential role under anaerobic conditions, as demonstrated here. Taken together, our results highlight that this pathway could be an interesting lead for the development of antibiotics targeting the denitrification metabolism.

RESULTS

UQ_9 is the major quinone of P. aeruginosa.

The quinone content of *P. aeruginosa* PAO1, grown under ambient air or anaerobic conditions (denitrification), was determined using electrochemical detection of lipid extracts separated by HPLC and compared to those obtained from *E. coli*. Whatever the conditions of growth, a major quinone species eluting at 11.5 min was present in the analyses of *P. aeruginosa* lipid extracts, UQ_{10} being used as standard (Fig. 1*A* and 1*B*). Mass spectrometry analysis showed a predominant ammonium adduct ($M+NH_4^+$) with *m/z* ratio of 812.7 (Fig. 1*C*), together with minor adducts such as Na^+ (817.6) and H^+ (795.7) (Fig. S1). These masses identify UQ_9 (monoisotopic mass 794.6) as the major quinone produced by *P. aeruginosa*. Membranes of *E. coli* contain UQ_8 and naphthoquinones (DMK_8 and MK_8). The absence of detectable level of naphthoquinones in *P. aeruginosa* lipid extracts, with or without oxygen (Fig.1*A* and 1*B*), is in agreement with the

absence of their biosynthetic pathways (MK or futalosine pathways) in *P. aeruginosa* genomes. It is also interesting to note that the UQ content of *E. coli* was higher under aerobic compared to anaerobic conditions (97±4 *versus* 42±6 pmol of UQ_8 per mg of cells), whereas we found the opposite for *P. aeruginosa* (95±4 *versus* 126±4 pmol of UQ_9 per mg of cells). Together, our results establish that UQ_9 is the major quinone of *P. aeruginosa* PAO1 and suggest that UQ_9 is used under denitrification conditions.

Identification of ubi genes in the genome of P. aeruginosa PAO1.

To identify the Ubi proteins of *P. aeruginosa*, IspB, UbiX, and UbiA to UbiK from *E. coli* MG1655 were first screened for homologs in the *P. aeruginosa* PAO1 protein sequence data set available at http://www.pseudomonas.com/ using the BLASTP software. As listed in Table S1, the analysis disclosed the presence of 11 homologous proteins (IspB, UbiA to UbiE, UbiG to UbiJ and UbiX). As reported previously, the functional homolog of UbiF is a Coq7-like hydroxylase (15) and the corresponding PA0655 protein was shown to be essential for aerobic UQ_9 biosynthesis (16). Overall, we propose that the O_2-dependent UQ biosynthetic pathways in *P. aeruginosa* and *E. coli* share a similar pattern (Fig. S2).

Under anaerobic conditions, *E. coli* still synthesizes UQ and we recently identified three genes that we called *ubiT*, *ubiV* and *ubiU*, as essential for this process (9). Homologues of *ubiT*, *ubiV* and *ubiU* were also identified in *P. aeruginosa* PAO1 and correspond to ORFs *PA3911*, *PA3912* and *PA3913*, respectively (Table S1 and Fig. S2). These genes were called hereafter $ubiT_{Pa}$, $ubiV_{Pa}$ and $ubiU_{Pa}$. The three genes are predicted to form an operon, *ubiUVT* (www.pseudomonas.com). Interestingly, this operon is located downstream of the genes *moeA1*, *moaB1*, *moaE*, *moaD* and *moaC* involved in the biosynthesis of the molybdopterin cofactor (MoCo) (Fig. 2), which is essential for nitrate reductase activity (17). Next, we evaluated the metabolic relevance of the O_2-independent UQ biosynthetic pathway in *P. aeruginosa* by studying mutants of $ubiT_{Pa}$, $ubiU_{Pa}$ and $ubiV_{Pa}$ genes.

Tn mutants of $ubiV_{Pa}$ and $ubiU_{Pa}$ present a growth defect for denitrification and an impaired UQ_9 content.

The physiological importance of the proteins $UbiT_{Pa}$, $UbiU_{Pa}$ and $UbiV_{Pa}$ was first investigated using transposon (Tn) mutants PW7609 ($ubiT_{Pa}$), PW7610 ($ubiV_{Pa}$), PW7611 ($ubiV_{Pa}$), PW7612 ($ubiU_{Pa}$) and PW7613 ($ubiU_{Pa}$) and the isogenic parental strain MPAO1 (wild-type strain from the Manoil collection) as control (Table S2). Aerobic growth in LB medium was similar between the Tn mutants and the wild-type strain MPAO1 (Fig. S3*A*) and the Tn mutants presented a UQ_9 level comparable to the wild-type (Fig. S3*B*). Thus, $UbiT_{Pa}$, $UbiU_{Pa}$ and $UbiV_{Pa}$ are not involved in the O_2-dependent UQ biosynthetic pathway of *P. aeruginosa*. In contrast, the growth of the $ubiV_{Pa}$ and $ubiU_{Pa}$ mutants was severely impaired in denitrification conditions (Fig. S3*C*) and their UQ_9 content was strongly lowered (Fig. S3*B*). These results suggest the overall requirement of $ubiU_{Pa}$ and $ubiV_{Pa}$ for denitrification in *P. aeruginosa*, supposedly *via* their involvement in O_2-independent UQ biosynthesis. Surprisingly, the growth of the $ubiT_{Pa}$ Tn mutant PW7609 was not affected (Fig. S3*C*) and it showed around 40% UQ_9 compared to the wild-type in anaerobic cultures (Fig. S3*B*). In this mutant, the Tn is inserted at the fifth base of the $ubiT_{Pa}$ gene, potentially leading to only partial inactivation of the gene (Table S2). We note that previous studies with *E. coli ubi* mutants showed that only 20% UQ was sufficient to maintain a wild-type growth phenotype (18,19).

Denitrification is dependent of $ubiT_{Pa}$, $ubiU_{Pa}$ and $ubiV_{Pa}$ genes via their involvement in O_2-independent UQ biosynthesis.

As $ubiT_{Pa}$, $ubiV_{Pa}$ and $ubiU_{Pa}$ are localized next to each other in the genome of PAO1, the transposon inserted in the mutants previously studied might impact the expression of the neighbouring genes. In addition, it is likely that the Tn mutant PW7609 is not disrupting properly the $ubiT_{Pa}$ gene. Thus, for each of the three genes, we constructed knockouts (KO) as well as complementation mutants in the parental strain PAO1. All deletion mutant strains (called hereafter *ubiTUV*-KO) shared a growth defect under denitrification coupled to a strong decrease of UQ_9 content compared to the wild-type (Fig. 3*A* and 3B), whereas UQ_9 content and growth were normal in aerobic conditions (Fig. 3*B* and 3*C*). In anaerobic conditions, *ubiTUV*-KO strains accumulated an early UQ biosynthetic intermediate corresponding to nonaprenylphenol (NPP) (Fig. S2 and Table S3). This result suggests that the O_2-independent UQ biosynthetic pathway

is blocked downstream of NPP in these three mutants. Interestingly, upon complementation, bacterial growth and UQ_9 levels were restored to those of the PAO1 strain used as control (Fig. 4*A*).

To confirm that UQ was directly involved in the restoration of the anaerobic growth of the *ubiTUV*-KO strains, UQ_4 solubilized in methanol was added to the denitrification medium at 5 and 50 µM final concentrations. After 24h of anaerobic incubation, colony-forming units per mL (CFU/mL) of each KO strain were estimated and compared to the same strain cultivated without UQ_4. The most significant results were obtained with 50 µM of UQ_4, which increased CFU of *ubiTUV*-KO strains by 8-15 fold (Fig. 4*B*). We noted a substantial toxicity of methanol on the wild-type strain (Fig. 4*B*, Ct lane), suggesting that the positive effect of UQ_4 on the *ubiTUV*-KO strains is likely underestimated. Taken together, our results show unequivocally that $UbiT_{Pa}$, $UbiU_{Pa}$ or $UbiV_{Pa}$ are needed for denitrification *via* their involvement in UQ biosynthesis.

$UbiT_{Pa}$, $UbiU_{Pa}$ and $UbiV_{Pa}$ are needed for the process of denitrification.

We used soft-agar experiments to examine dioxygen and nitrate requirements of *ubiTUV*-KO strains with or without the wild-type allele. Soft agar was prepared anaerobically in LB medium containing KNO_3 at 100 mM final concentration and then exposed to ambient air. Oxygen diffuses through the agar to form a gradient, the highest concentration being at the top of the agar (Fig. 4*C*, lane 1). As shown in Fig. 4*C*, parental strain PAO1 and complemented *ubiTUV*-KO strains grew throughout the tube because they were able to use aerobic respiration as well as denitrification. In contrast, the growth of the *ubiTUV*-KO strains harboring the empty vector was restricted to the oxygenated part of the medium, whereas the presence of the respective genes on the plasmids allowed growth in the anaerobic medium (Fig. 4*C*). The bubbles observed in the soft agar correspond to gas evolution of N_2O and/or N_2 (12), suggesting a restoration of the denitrification process in the lower part of the tube. Taken together, these results point to the requirement for *$ubiT_{Pa}$*, *$ubiU_{Pa}$* and *$ubiV_{Pa}$* beyond the nitrate reduction step and support that UQ is probably essential for the entire denitrification process in *P. aeruginosa*.

Molybdopterin cofactors are not involved in anaerobic UQ_9 biosynthesis.

As mentioned previously, the *ubiUVT* operon is located downstream of the genes *moeA1*, *moaB1*, *moaE*, *moaD* and *moaC* involved in MoCo biosynthesis. Currently, MoCo-containing hydroxylases constitute the only family known to catalyze O_2-independent hydroxylation reactions (20). Since three O_2-independent hydroxylation reactions are needed to synthesize UQ anaerobically and that UbiU and UbiV are suspected to be involved in these reactions (9), we reasoned that MoCo might be involved in this process, providing a rationale for the co-localization of the *ubi* and *moa/moe* genes. To test this hypothesis, we evaluated the ability of Tn mutants PW7614, PW7615/PW7616, PW7618/PW2470, PW7619/PW1920 and PW7621/PW7622 (Table S2) corresponding respectively to Tn insertions in the ORFs *moeA1*, *moaB1* (two mutants), *moaE* (two mutants), *moaD* (two mutants) and *moaC* (two mutants) to synthesize UQ_9 without O_2. However, MoCo is also essential for nitrate reductase activity and thus for denitrification (17). To overcome this problem, WT and Tn mutants were grown in LB medium using arginine as a fermentable energy source in rich medium. As expected, all the Tn mutants exhibited a growth defect in denitrification. However, anaerobic growth was rescued by addition of arginine as previously described (21), and we were therefore able to measure the UQ content of the cells in these conditions (Fig. S4). The UQ_9 content of the MoCo Tn mutants was comparable to that of the wild-type strain (Fig. S4), suggesting that MoCo is not involved in anaerobic UQ_9 biosynthesis.

Recombinant $UbiV_{Pa}$ is an air-sensitive [4Fe-4S] cluster-containing protein.

To gain insights into their biochemical properties, we produced and purified the three proteins in *E. coli*, $UbiV_{Pa}$ being the most soluble. First, we showed that $UbiV_{Pa}$ purified by size exclusion chromatography (SEC) behaved as a monomer (Fig. S5*A* and S5*B*). Moreover, we noticed that the fraction containing the purified protein was slightly pink-colored with a UV-visible absorption spectrum characteristic of the presence of iron-sulfur species (22), with a band at 410 nm and broad and low intensity shoulders between 450 and 600 nm (Fig. 5*A*, dotted line) (23). However, the amount of iron and sulfur (0.22 iron and 0.22 sulfur/monomer) was largely substoïchiometric, suggesting a degradation of the [Fe-S] cluster during the purification of the protein under aerobic conditions, as already

observed for many other Fe-S proteins. Consistent with this hypothesis, anaerobic reconstitution of the [Fe-S] cluster allowed to obtain a brown color protein with a UV-visible spectrum displaying one broad absorption band at 410 nm, which is characteristic of a $[4Fe\text{-}4S]^{2+}$ cluster (Fig. 5*A*, solid line) (24). The iron and sulfide determination yielded 3.90 ± 0.03 iron and 3.40 ± 0.20 sulfur/monomer of $UbiV_{Pa}$, consistent with the presence of one [4Fe-4S] cluster/protein (Table 1). As shown in Fig. S5*C*, the [Fe-S] cluster of $UbiV_{Pa}$ was sensitive to air.

Four strictly conserved cysteines (C39, C180, C193, and C197) arranged in a $CX_nCX_{12}CX_3C$ motif (X representing any amino acid) are found in $UbiV_{Pa}$ (9). To test if these four cysteines are important for the chelation of the [4Fe-4S] cluster present in $UbiV_{Pa}$, we generated two double mutants (C39AC180A and C193AC197A) and a triple mutant (C39AC193AC197A). All these mutants were colorless after purification under aerobic conditions and did not show any absorption band in the 350- to -550-nm region of their UV-Vis spectra (Fig. S5*D*), suggesting that they were impaired in their capacity to accommodate a [Fe-S] cluster. After reconstitution under anaerobic conditions, $UbiV_{Pa}$ C39AC193AC197A precipitated and its UV-vis spectrum could not be recorded. Although they also had a tendency to aggregate, 10% of the double mutants behaved as monomers permitting some assays. Overall, their absorbance at 410 nm (Fig. 5*B*) and their iron and sulfur contents (Table 1) were largely decreased compared to the wild-type protein, suggesting that the four conserved cysteines are good candidates as ligands of the [4Fe-4S] cluster present in $UbiV_{Pa}$.

Recombinant $UbiU_{Pa}$ and $UbiT_{Pa}$ co-purify with UQ_8 in *E. coli*.

We have recently demonstrated that isoprenoid quinones were able to co-elute with the Ubi-proteins such as UbiJ (11) and that UbiT exhibits a sterol carrier protein 2 (SCP2) domain, which is able to bind lipids (9). To that end, we performed lipid content analysis of the $UbiT_{Pa}$, $UbiU_{Pa}$ and $UbiV_{Pa}$ fractions purified from *E. coli* extracts. No isoprenoid quinones were detected co-eluting with $UbiV_{Pa}$ (Table S4). In contrast, UQ_8 and DMQ_8 (2-octaprenyl-3-methyl-6-methoxy-1,4-benzoquinone) were shown to co-purify with $UbiU_{Pa}$. This protein was purified only in the presence of detergent, as it was insoluble without it. After a two-step purification protocol, including a Ni-NTA chromatography and a SEC, the solubilized protein had still a tendency to form different oligomeric states covering the fractions 14 to 44 as shown in Fig. 6*A* and 6*B*. UQ_8 and DMQ_8 were mainly detected in the elution fractions 33 to 45 (Fig. 6*A*) corresponding to only a proportion of the purified $UbiU_{Pa}$ (Fig. 6*B*). The highest contents, i.e. 488.17 pmoles of UQ_8 per mg of protein and 19 932 AU of DMQ_8 per mg of protein, were assayed in the fraction 39 and 40, respectively (Table S4). This corresponds to a UQ_8/protein ratio of 1.5%. Taken together, these results show that UQ_8 and DMQ_8 co-purify with $UbiU_{Pa}$ depending of its oligomerization state.

Due to a lack of solubility, $UbiT_{Pa}$ was overproduced with *E. coli* thioredoxin (TrxA) as a gene fusion partner, as previously described (25). After the first step of the purification process (Ni-NTA chromatography), the 32 kDa TrxA-$UbiT_{Pa}$ fusion protein was digested with thrombin. Then in order to remove the TrxA His-tagged protein, $UbiT_{Pa}$ was purified by Ni-NTA chromatography coupled to SEC, as a high oligomeric form (Fig. 6*C*). The purified $UbiT_{Pa}$ (pool of fractions 20 to 30) contained 9.75±4.57 pmoles of UQ_8 per mg of protein (Table S4), which corresponds to a UQ_8/protein ratio of about 0.03%.

Recombinant $UbiU_{Pa}$ and $UbiT_{Pa}$ bind the isoprenoid tail of UQ.

To further confirm the ability of $UbiT_{Pa}$ and $UbiU_{Pa}$ to bind UQ, a protein-lipid overlay assay was performed (Fig. 6*D*). We checked the possibility of these proteins to recognize UQ_{10}, UQ_8, solanesol, 3-methylcatechol, 1-palmitoyl-2-oleoyl-*sn*-glycero-3-phosphoethanolamine (POPE) and cholesterol. Solanesol is a non-cyclic terpene alcohol that consists of nine isoprene units as found in UQ_9. 3-methylcatechol was chosen to mimic the head group of UQ. POPE is the major lipid component of the inner membrane of *E. coli* (26). Finally, cholesterol was used as a sterol standard. Fig. 6*D* shows that $UbiT_{Pa}$, and $UbiU_{Pa}$ did not interact with 3-methylcatechol, POPE, or cholesterol in our experimental conditions. In contrast, both proteins were able to recognize UQ_{10}, UQ_8 and solanesol. We established the ability of $UbiT_{Pa}$ to bind phosphatidic acid (PA) as previously demonstrated by Groenewold *et al*. (25) (Fig. S6). Together, we show that $UbiT_{Pa}$ and $UbiU_{Pa}$ are able to bind the isoprenoid tail of UQ in agreement with their involvement in the O_2-independent biosynthetic pathway of UQ.

DISCUSSION

UQ acts as a membrane-embedded electron and proton shuttle and is a key molecule in the respiratory metabolism of proteobacteria. Biosynthesis of UQ in aerobic conditions has been widely studied and includes a series of enzymatic reactions in which a benzene ring undergoes a series of modifications involving a prenylation, a decarboxylation, three methylations, and three hydroxylations (27). Our chemical analysis identified UQ_9 as the major quinone in the membranes of aerobically grown *P. aeruginosa* cells, which is in agreement with the literature (7,16). We found in *P. aeruginosa* homologues of the genes known to be involved in UQ biosynthesis in *E. coli*, except *ubiF* (Table S1). Indeed, as already published, *P. aeruginosa* exhibits a yeast COQ7 protein homolog, which catalyzes the same reaction as UbiF from *E. coli* (15,16). Thereby, both bacteria share a similar UQ biosynthetic pathway involving three hydroxylases - UbiI, UbiH and UbiF or COQ7 - using O_2 as a co-substrate (Fig. S2). As no other isoprenoid quinone was detected in lipid extracts of *P. aeruginosa*, we suppose that UQ_9 is essential for aerobic growth of this bacterium.

In the absence of oxygen, *P. aeruginosa* can grow by dissimilatory nitrate respiration by using nitrate or nitrite as alternative terminal electron acceptors of the respiratory chain. This metabolic process, known as denitrification, has been widely studied (3). However, the component acting to transfer electrons from primary dehydrogenases to nitrate or nitrite reductases was not clearly identified to date (3). In the present study, we identified UQ_9 as the major quinone synthesized in anaerobic conditions. By LC-MS analysis, we also identified two related redox molecules, UQ_8 and DMQ_9 present in small amounts (see Fig. 1B, the peaks around 8 and 9.5 min) and nonaprenylphenol (NPP, see Fig. S2). NPP and DMQ_9 are UQ_9 biosynthetic intermediates (see Fig. S2) and UQ_8 was already detected in *Pseudomonas* lipid extracts in aerobic conditions (16). Taken together, these results suggest that *P. aeruginosa* possesses an O_2-independent UQ biosynthetic pathway, which produces the major quinone species observed under anaerobic conditions. We recently identified such pathway in *E. coli* (9). Here, we characterized three genes, $ubiT_{Pa}$ *(PA3911)*, $ubiU_{Pa}$ *(PA3913)* and $ubiV_{Pa}$ *(PA3912) as* essential for the anaerobic UQ_9 biosynthesis in *P. aeruginosa* and dispensable for the aerobic one. These genes are homologs to the *ubiT*, *ubiU* and *UbiV* previously identified in *E. coli*, which grows normally in anaerobic conditions in a UQ-independent manner because of the presence of naphthoquinones (9) (28) (29). In contrast, we demonstrated that these three genes were essential to anaerobic denitrification metabolism of *P. aeruginosa*, which is in agreement with the presence of a single quinone corresponding to UQ. In line with our results, $ubiV_{Pa}$ (*PA3912*) and $ubiU_{Pa}$ (*PA3913*) are expressed in response to anaerobic conditions (30) and the abundance of $UbiU_{Pa}$ protein was increased during anaerobic growth (31). Moreover, using random transposon mutagenesis, $ubiV_{Pa}$ (*PA3912*) and $ubiU_{Pa}$ (*PA3913*) were already reported as essential for anaerobic growth of *P. aeruginosa* on nitrate and nitrite as alternative terminal electron acceptors of the respiratory chain (21).

Although its contribution is still poorly understood for within-host growth, anaerobic respiration of *P. aeruginosa* is likely to be significant for promoting virulence mechanisms in chronic lung infections (13). Indeed, the infected endobronchial mucus of CF patients is subject to severe hypoxia or even anoxia (32). A likely hypothesis is that accelerated O_2 consumption in the biofilm may result from activated polymorphonuclear leukocytes that produce superoxide (33) and nitric oxide (34). Indeed, high levels of nitrate and nitrite have been measured in sputum from CF patients (35). From all these observations and as UQ is an essential component of the denitrification metabolism in *P. aeruginosa*, we propose that $UbiT_{Pa}$, $UbiV_{Pa}$ and $UbiU_{Pa}$ may contribute to the CF lung infection in patients (work in progress in our laboratory). This hypothesis is supported by a recent quantitative proteomics approach revealing increased abundance of the three proteins in anaerobic biofilms grown under conditions of the cystic fibrosis lung (25). Moreover, deduced from a high-throughput sequencing of Tn libraries from *P. aeruginosa* strain PA14, it appears that *ubiT* gene was found to be essential for this bacterium to colonize the murine gastrointestinal tract (36), which suggests that O_2-independent UQ biosynthesis could be essential for bacterial virulence. This hypothesis is also supported by the essential contribution of UbiU and UbiV homologs to *Yersinia ruckeri* virulence (37).

As already suggested, homologs of UbiU and UbiV would belong to a new family of O_2-independent hydroxylases (9). To date, only the

MoCo-containing hydroxylases using water-derived oxygen are known to catalyze hydroxylations in anaerobic conditions (20). In our study, we have demonstrated that MoCo is not essential to the anaerobic UQ pathway, strengthening the hypothesis that hydroxylation reactions performed in UbiU- and UbiV-dependent manner do not involve MoCo.

In order to better understand their functions, we decided to overproduce in *E. coli*, purify and biochemically characterize $UbiT_{Pa}$, $UbiU_{Pa}$ and $UbiV_{Pa}$. Our results showed that recombinant $UbiV_{Pa}$ is an air-sensitive Fe-S containing protein, as UbiV from *E. coli* (9), and we demonstrated that cysteines 39, 180, 193 and 197 were ligands to the [4Fe-4S] cluster found in $UbiV_{Pa}$. These results confirm the conservation of a four cysteines pattern coordinating a Fe-S cluster across homologs of UbiV. This pattern is also found in RlhA and TrhP (38,39), two proteins that belong to the same proteases U32 family than UbiU and UbiV, and that are also involved in O_2-independent hydroxylation reactions in *E. coli* (38,39). However, the function of the iron-sulfur centers in the hydroxylation mechanism remains to be understood.

As a member of the U32 protease family, $UbiU_{Pa}$ also presents four conserved cysteines (C169, C176, C193 and C232). Unfortunately, we failed to reconstitute a Fe-S cluster and obtained instead protein precipitation. Indeed, $UbiU_{Pa}$ is an unstable protein. Unlike UbiU from *E. coli*, which forms a stable heterodimer UbiU-UbiV complex (9), we were not able to solubilize $UbiU_{Pa}$ by co-producing it with its potential partner $UbiV_{Pa}$. The fact that we produced *P. aeruginosa* proteins in *E.coli* could explain this difference in behavior. Nevertheless, an UbiU-UbiV complex in *P. aeruginosa* remains a reasonable hypothesis that needs further investigations. We were able to purify $UbiU_{Pa}$ alone with significant quantities of UQ_8 and DMQ_8, whereas purified $UbiV_{Pa}$ contained no quinones. This result was confirmed by a protein-lipid overlay assay, which showed that the isoprenoid tail of UQ was the structural determinant for the recognition by $UbiU_{Pa}$. From these results, we propose that UbiU would bind UQ and reaction intermediates of the anaerobic UQ pathway.

Homologs of UbiT and UbiJ contain a SCP2 domain (9,40), involved in protein-lipid interactions and UbiJ from *E. coli* co-purified with UQ_8 (11). Moreover, a previous study showed that PA3911 ($UbiT_{Pa}$) was able to bind specifically PA, the central hub of phospholipid metabolism (25). Here we showed that $UbiT_{Pa}$ binds to UQ_8 and shares with $UbiU_{Pa}$ the recognition of the isoprenoid tail of UQ. Taken together, these results support the hypothesis that UbiT may be the counterpart of UbiJ in anaerobic conditions. We propose that UbiT may bind UQ intermediates and may stabilize a putative anaerobic Ubi complex that has yet to be demonstrated.

EXPERIMENTAL PROCEDURES

Bacterial strains and growth conditions.

P. aeruginosa and *E. coli* strains used in this study are listed in Table S2. We obtained the collection of transposon (Tn) mutants in *P. aeruginosa* MPAO1 strain from the Manoil Laboratory, Department of Genome Science, University of Washington, USA (41,42). The Tn insertion site of the mutant strains were verified by sequencing (GATC Biotech, Konstanz, Germany) using PCR primers recommended by the library curators. *P. aeruginosa* strains were aerobically maintained at 37°C on lysogeny broth (LB) agar plates. For quinone assay, aerobic cultures (5 mL) were performed in LB medium at 37°C with rotary shaking at 200 rpm. Anaerobic growth of *P. aeruginosa* were performed in a 12 mL Hungate tubes containing LB medium supplemented with KNO_3 as an electron acceptor (100 mM final concentration) (43), hereafter called denitrification medium, and deoxygenated 30 min by argon bubbling (O_2<0.1 ppm) prior to autoclaving. In some experiments, LB medium was supplemented with arginine at a final concentration of 40 mM instead of KNO_3 (44). Hungate tubes were inoculated through the septum with 100 µL of overnight cultures taken with disposable syringe and needles from closed Eppendorf tubes filled to the top. Cultures in Hungate tubes were used for measuring the quinone contents. For aerobic growth studies, aerobic overnight cultures were used to inoculate a 96-well plate to obtain a starting optical density at 600 nm (OD_{600}) of 0.05 and further incubated with shaking at 37°C. Changes in OD_{600} were monitored every 10 min for 12 h using the Infinite 200 PRO microplate reader (Tecan, Lyon, France). For anaerobic growth curve studies, overnight cultures in 50 mL closed tubes of not degassed denitrification medium were used to inoculate 400 mL bottles to obtain a starting OD_{600} of 0.05. Then, bacteria were grown anaerobically by sparging argon (O_2<0.1 ppm) and bacterial cultures were monitored

spectrophotometrically (OD_{600}) at 30 min intervals for 9h. *E. coli* MG1655 and DH5α were grown on LB agar or in LB liquid. When required, the medium was supplemented with ampicillin at 100 µg/mL for *E. coli*, carbenicillin at 250 µg/mL for *P. aeruginosa*, or tetracycline at 60 µg/mL for *E. coli* and 100 µg/mL for *P. aeruginosa* or gentamicin at 200 µg/mL for *P. aeruginosa* (Table S2). When necessary, UQ_4 or 0.1% (w/v) arabinose final concentration was added to the medium to enhance bacterial anaerobic growth or to induce P_{BAD} expression of pSW196-derived plasmids, respectively. *Pseudomonas* Isolation Agar (PIA) medium (from DB) containing irgasan (25 µg/L) was used for triparental mating to counter select *E. coli*. For CFU counting, bacteria were suspended in PBS and cell suspensions were serially diluted in PBS. For each sample, 100 µL of at least four different dilutions were plated on LB plates, incubated for 24 h at 37°C and CFU were counted using a Scan 100 Interscience.

Plasmids and genetic manipulations.

The plasmids and the primers used in this study are listed in Tables S2 and S4). All the plasmids produced in this work were checked using DNA sequencing (GATC Biotech, Konstanz, Germany). To generate *P. aeruginosa* deletion mutants, overlapping upstream and downstream flanking regions of *ubiT*$_{Pa}$, *ubiU*$_{Pa}$ and *UbiV*$_{Pa}$ genes were obtained by PCR amplification using PAO1 genome as template and the oligonucleotides described in Table S5. The resulting fragments were then cloned into *Sma*I-cut pEXG2 plasmid by sequence and ligation-independent cloning (45). To complement the mutants, the *ubiT*$_{Pa}$, *ubiU*$_{Pa}$ and *ubiV*$_{Pa}$ fragments were generated by PCR amplification using the oligonucleotide pairs ubiT-PA-F/ubiT-PA-R, ubiU-PA-F/ubiU-PA-R and ubiV-PA-F/ubiV-PA-R, respectively, and PAO1 genome as template (Table S5). The fragments were *Eco*RI-*Sac*I digested and inserted into P_{BAD}-harboring pSW196 plasmid, yielding the p*ubiT*$_{Pa}$, p*ubiU*$_{Pa}$ and p*ubiV*$_{Pa}$ plasmids, respectively (Table S2). The pEXG2- and pSW196-derived vectors were transferred into *P. aeruginosa* PAO1 strain by triparental mating using pRK2013 as a helper plasmid (46). For allelic exchange using the pEXG2 plasmids, co-integration events were selected on PIA (*Pseudomonas* Isolation Agar) plates containing gentamicin. Single colonies were then cultured on NaCl-free LB agar plates containing 10% (w/vol) sucrose to select for the loss of the plasmid, and the resulting sucrose-resistant colonies were checked for mutant genotype by PCR. To overproduce C-terminally His-tagged $UbiV_{Pa}$, the *ubiV*$_{Pa}$ gene was cloned into the pET22b(+) vector. The *ubiV*$_{Pa}$ insert was obtained by PCR amplification using the oligonucleotide pair pET22-UbiV-F and pET22-UbiV-R and *ubiV*$_{Pa}$ ORF as template (Table S5). *Nde*I-*Xho*I digested amplicon was ligated to *Nde*I-*Xho*I digested pET22b(+) vector to obtain pET22-$UbiV_{Pa}$ (Table S2). Variants of $UbiV_{Pa}$ were obtained using the Q5 Site-Directed Mutagenesis Kit (New England Biolabs) ($UbiV_{Pa}$ C193AC197A and $UbiV_{Pa}$ C39AC193AC197A) and the QuickChange II XL Site-Directed Mutagenesis Kit (Agilent) ($UbiV_{Pa}$ C39AC180A) according to the manufacturer's specifications using pET22b-$UbiV_{Pa}$ as template (Table S2 and S5). The *ubiU*$_{Pa}$ gene was cloned into pET-22b(+) by following the same protocol as that for *ubiV*$_{Pa}$ gene. The *ubiT*$_{Pa}$ gene was synthesized by Eurofins with *E. coli* codon optimization. The synthetic gene was then cloned into the EcoRI/NotI sites of vector pET32a(+) (Novagen), resulting in plasmid pET32-TrxA-$UbiT_{Pa}$ (Table S2).

Soft-agar study to evaluate the O_2-dependency of growth.

Soft-agar studies were performed in denitrification medium supplemented by agar 0.7% (w/v) final concentration. After argon bubbling (O_2<0.1 ppm) for 30 min, the suspension (13 mL) was autoclaved in Hungate tubes. They were then placed in a 40°C incubator and they were inoculated through the septum with 100 µL of overnight cultures taken with disposable syringe and needles from Eppendorf tubes filled to the top, mixed by inverting, and incubated at room temperature 30 min to allow the agar to solidify. Then, the tubes were incubated under aerobic conditions with caps loosened at 37°C for 24 h. A control experiment was performed with resazurin (0.25 µg/mL final concentration) used as an indicator of medium oxygenation. When required, the medium was supplemented with antibiotics.

Lipid extractions and quinone analysis.

Cultures (5 mL under ambient air and 13 mL under anaerobic conditions) were cooled down on ice before centrifugation at 3200 g, 4°C, 10 min. Cell pellets were washed in 1 mL ice-cold PBS and transferred to pre-weighted 1.5 mL Eppendorf tubes. After centrifugation at 12 000 g,

4°C, 1 min and elimination of supernatant, the cell wet weight was determined (~5-30 mg) and pellets were stored at -20°C. Quinone extraction from cell pellets was performed as previously described (18). Lipid extracts corresponding to 1 mg of cell wet weight were analyzed by HPLC electrochemical detection-mass spectrometry (ECD-MS) with a BetaBasic-18 column at a flow rate of 1 mL/min with mobile phases composed of methanol, ethanol and a mix of 90% isopropanol, 10% ammonium acetate (1 M), 0.1% TFA: mobile phase 1 (50% methanol, 40% ethanol and 10% mix). When necessary, MS detection was performed on a MSQ spectrometer (Thermo Scientific) with electrospray ionization in positive mode (probe temperature 400°C, cone voltage 80V). Single ion monitoring (SIM) detected the following compounds: UQ_8 ($M+NH_4^+$), m/z 744-745, 6-10 min, scan time 0.2 s; UQ_9 ($M+NH_4^+$), m/z 812-813, 9-14 min, scan time 0.2 s; UQ_{10} ($M+NH_4^+$), m/z 880.2-881.2, 10-17 min, scan time 0.2 s., DMQ_8 ($M+NH_4^+$), m/z 714-715, 5-10 min, scan time 0.2 s and NPP ($M+NH_4^+$), m/z 724-725, 8-13 min, scan time 0.2 s. MS spectra were recorded between m/z 600 and 900 with a scan time of 0.3 s. ECD and MS peak areas were corrected for sample loss during extraction on the basis of the recovery of the UQ_{10} internal standard and were then normalized to cell wet weight. The peaks of UQ_8 and UQ_9 obtained with electrochemical detection were quantified with a standard curve of UQ_{10} as previously described (18).

Overproduction and purification of UbiV, UbiU and UbiT from P. aeruginosa in E. coli.

Wild-type and variants $UbiV_{Pa}$ were expressed and purified as previously described for *E. coli* proteins (9). Briefly, the pET-22b(+) plasmid, encoding wild-type or variants $UbiV_{Pa}$, were co-transformed with pGro7 plasmid (Takara Bio Inc.) into *E. coli* BL21 (DE3) Δ*ubiUV* competent cells grown at 37 °C in LB medium, which was supplemented with ampicillin (50 µg/mL), kanamycin (50 µg/mL) and chloramphenicol (12.5 µg/mL). At an OD_{600} = 1.2, D-arabinose was added to the cultures at a final concentration of 2 mg/mL. At an OD_{600} = 1.8, cultures were cooled down on ice for 20 min, and IPTG was added at a final concentration of 0.1 mM. Cells were then allowed to grow further at 16 °C overnight. Wild-type $UbiV_{Pa}$ and the different variants were purified by Ni-NTA chromatography followed by SEC in buffer A (50 mM Tris-HCl, 25 mM NaCl, 15% (v/v) glycerol, pH 8.5) containing 1 mM DTT. The purified proteins were concentrated to 30-40 mg/mL using Amicon concentrators (30-kDa cutoff; Millipore).

The overproduction of wild-type $UbiU_{Pa}$ was performed in *E. coli* BL21 (DE3) Δ*ubiUV* cells by following the same protocol as that for $UbiV_{Pa}$, except that $UbiU_{Pa}$ over-expression was induced with 0.05 mM of IPTG and the cell pellets were resuspended in buffer B (50 mM Tris-HCl, 500 mM NaCl, 15% (v/v) glycerol, pH 8.5) containing 0.2% (w/v) N-lauroylsarcosine sodium salt. After cell disruption by sonication, the clarified cell-free extracts were loaded onto a His-Trap FF crude column (GE Healthcare) pre-equilibrated with buffer B containing 0.1% (w/v) N-lauroylsarcosine sodium salt. The column was washed with 10 column volumes of buffer C (50 mM Tris-HCl, 500 mM NaCl, 15% (v/v) glycerol, 10 mM imidazole, pH 8.5) containing 6 mM N,N-dimethyldodecylamine N-oxide (LDAO) to remove non-specifically bound *E. coli* proteins and then eluted with a linear gradient of 10 column volumes of buffer C containing 500 mM imidazole and 6 mM LDAO. Fractions containing $UbiU_{Pa}$ were pooled and then loaded on a HiLoad 16/600 Superdex 200 pg (GE Healthcare) pre-equilibrated in buffer D (50 mM Tris-HCl, 150 mM NaCl, 15% (v/v) glycerol, pH 8.5) containing 3 mM LDAO. The purified proteins were concentrated using Amicon concentrators (100-kDa cutoff; Millipore), aliquoted, frozen in liquid nitrogen, and stored at -80°C. For protein-lipid overlay, fractions 34-43 were pooled.

Overproduction of $UbiT_{Pa}$ fused with the thioredoxin (TrxA-$UbiT_{Pa}$) in *E. coli* BL21 (DE3) Δ*ubiUV* cells was performed by following the same protocol as that for $UbiU_{Pa}$, except that over-expression of chimeric gene was induced at an OD_{600} of 0.5 and the cell pellet was resuspended in buffer B containing 5% (w/v) sodium cholate. TrxA-$UbiT_{Pa}$ was first purified, following the same protocol as that for $UbiU_{Pa}$, by Ni-NTA chromatography, except that the HisTrap FF crude column was pre-equilibrated with buffer B containing 0.5% (w/v) sodium cholate and then eluted with buffer C containing 500 mM imidazole and 0.5% (w/v) sodium cholate. Fractions containing TrxA-$UbiT_{Pa}$ were pooled and detergent was removed using a Hiprep 26/10 Desalting column (GE Healthcare) preequilibrated with buffer D. The fusion protein was digested with thrombin (10 units/mg of TrxA-$UbiT_{Pa}$) at room temperature and then loaded on a HiLoad 16/600 Superdex 200 pg (GE Healthcare) coupled with a HisTrap FF crude

column (GE Healthcare) pre-equilibrated with buffer D. The purified proteins were concentrated using Amicon concentrators (100-kDa cutoff; Millipore), aliquoted, frozen in liquid nitrogen, and stored at -80°C.

[Fe-S] cluster reconstitution.

The [Fe-S] cluster(s) of holo-UbiV_{Pa} and holo-variants was reconstituted as previously described (9). Briefly, a solution containing 100 µM of as-purified proteins was treated with 5 mM DTT for 15 min at 20°C and then incubated for 1 h with a 5-fold molar excess of both ferrous ammonium sulfate and L-cysteine. The reaction was initiated by the addition of a catalytic amount of the *E. coli* cysteine desulfurase CsdA (1-2% molar equivalent) and monitored by UV-visible absorption spectroscopy. After 1 h of incubation, the holo-proteins were then loaded onto a Superdex 75 Increase 10/300 GL column (GE Healthcare) pre-equilibrated with buffer A. The fractions containing the holo-proteins were pooled and concentrated to 20-30 mg/mL on a Vivaspin concentrator (30-kDa cutoff).

Protein-lipid overlay.

To assess the lipid-binding properties of UbiT_{Pa} and UbiU_{Pa}, a protein–lipid overlay was performed as previously described (47). Briefly, 2 µL of 20 mM lipids in dichloromethane were spotted onto PVDF membrane and allowed to dry at room temperature for 1 h. The membranes were blocked in 3 % (w/v) fatty acid-free BSA in TBST (50 mM Tris-HCl, 150 mM NaCl and 0.1% (v/v) Tween-20, pH 7.5) for 1 h. The membranes were then incubated overnight at 4 °C with gentle stirring in the same solution containing 0.2 µg/mL of the indicated proteins. After washing six times during 30 min in TBST buffer, the membranes were incubated for 1 h with a 1/1000 dilution of anti-polyHis monoclonal antibody (Sigma) and then for 1 h with a 1/10 000 dilution of anti-mouse–horseradish peroxidase conjugate (Thermo Fisher Scientific). His-tagged proteins bound to the membrane by virtue of its interaction with lipid, were detected by enhanced chemiluminescence using Clarity Max Western ECL Substrate (Bio-rad).

Quantification methods.

Protein concentrations were determined using the method of Bradford (Bio-Rad) with bovine serum albumin as the standard. The iron and acid-labile sulfide were determined according to the method of Fish (48) and Beinert (49), respectively, before and after [4Fe-4S] cluster reconstitution**.**

UV-vis spectroscopy.

UV-visible spectra were recorded in 1-cm optic path quartz cuvettes under aerobic conditions on a Cary 100 Uv-vis spectrophotometer (Agilent) and under anaerobic conditions in a glove box on a XL-100 Uvikon spectrophotometer equipped with optical fibers.

The abbreviations used are: MK, menaquinone; UQ, ubiquinone; DMK, dimethyl-menaquinone; DMQ, C6-demethoxy-ubiquinone; NPP, nonaprenylphenol; SEC, size exclusion chromatography; SCP2, sterol carrier protein 2; IPTG, isopropyl-1-thio-β-D-galactopyranoside; ECD, electrochemical detection; PA: phosphatidic acid; POPE: 3-methylcatechol, 1-palmitoyl-2-oleoyl-*sn*-glycero-3-phosphoethanolamine.

Author contributions: L. P., F. B., M. F., M. L. conceived and designed the experiments. C. -D. -T., J. M., S. E., E. B., and L. P. performed the experiments. E. B. and B. F. contributed reagents/materials/analysis tools. L. P., M. L., and F. P. wrote the paper. All authors analyzed the results and approved the final version of the manuscript.

Acknowledgements: This work was supported by the Agence Nationale de la Recherche (ANR), projects (An)aeroUbi ANR-15-CE11-0001-02, O_2-taboo ANR-19-CE44-0014, DYNAMO ANR-11-LABX-0011-01 and ANR-10-LABX-62-IBEID, the University Grenoble Alpes (UGA), the French Centre National de la Recherche Scientifique (CNRS) and the Commissariat à l'Energie Atomique et aux Energies Alternatives (CEA)

Competing interests: The authors declare that they have no competing interests.

Data availability: All data is contained within the manuscript and supplemental materials.

REFERENCES

1. Crull, M. R., Somayaji, R., Ramos, K. J., Caldwell, E., Mayer-Hamblett, N., Aitken, M. L., Nichols, D. P., Rowhani-Rahbar, A., and Goss, C. H. (2018) Changing Rates of Chronic *Pseudomonas aeruginosa* Infections in Cystic Fibrosis: A Population-Based Cohort Study. *Clin Infect Dis* **67**, 1089-1095
2. Magill, S. S., Edwards, J. R., Bamberg, W., Beldavs, Z. G., Dumyati, G., Kainer, M. A., Lynfield, R., Maloney, M., McAllister-Hollod, L., Nadle, J., Ray, S. M., Thompson, D. L., Wilson, L. E., Fridkin, S. K., Emerging Infections Program Healthcare-Associated, I., and Antimicrobial Use Prevalence Survey, T. (2014) Multistate point-prevalence survey of health care-associated infections. *N Engl J Med* **370**, 1198-1208
3. Arai, H. (2011) Regulation and Function of Versatile Aerobic and Anaerobic Respiratory Metabolism in *Pseudomonas aeruginosa*. *Front Microbiol* **2**, 103
4. Williams, H. D., Zlosnik, J. E., and Ryall, B. (2007) Oxygen, cyanide and energy generation in the cystic fibrosis pathogen *Pseudomonas aeruginosa*. *Adv Microb Physiol* **52**, 1-71
5. Torres, A., Kasturiarachi, N., DuPont, M., Cooper, V. S., Bomberger, J., and Zemke, A. (2019) NADH Dehydrogenases in *Pseudomonas aeruginosa* Growth and Virulence. *Front Microbiol* **10**, 75
6. Page, A. C., Jr., Gale, P., Wallick, H., Walton, R. B., Mc, D. L., Woodruff, H. B., and Folkers, K. (1960) Coenzyme Q. 17. Isolation of coenzyme Q10 from bacterial fermentation. *Arch Biochem Biophys* **89**, 318-321
7. Matsushita, K., Yamada, M., Shinagawa, E., Adachi, O., and Ameyama, M. (1980) Function of ubiquinone in the electron transport system of *Pseudomonas aeruginosa* grown aerobically. *J Biochem* **88**, 757-764
8. Nowicka, B., and Kruk, J. (2010) Occurrence, biosynthesis and function of isoprenoid quinones. *Biochim Biophys Acta* **1797**, 1587-1605
9. Pelosi, L., Vo, C. D., Abby, S. S., Loiseau, L., Rascalou, B., Hajj Chehade, M., Faivre, B., Gousse, M., Chenal, C., Touati, N., Binet, L., Cornu, D., Fyfe, C. D., Fontecave, M., Barras, F., Lombard, M., and Pierrel, F. (2019) Ubiquinone Biosynthesis over the Entire O2 Range: Characterization of a Conserved O2-Independent Pathway. *mBio* **10**
10. Alexander, K., and Young, I. G. (1978) Alternative hydroxylases for the aerobic and anaerobic biosynthesis of ubiquinone in *Escherichia coli*. *Biochemistry* **17**, 4750-4755
11. Hajj Chehade, M., Pelosi, L., Fyfe, C. D., Loiseau, L., Rascalou, B., Brugiere, S., Kazemzadeh, K., Vo, C. D., Ciccone, L., Aussel, L., Coute, Y., Fontecave, M., Barras, F., Lombard, M., and Pierrel, F. (2019) A Soluble Metabolon Synthesizes the Isoprenoid Lipid Ubiquinone. *Cell Chem Biol* **26**, 482-492 e487
12. Zumft, W. G. (1997) Cell biology and molecular basis of denitrification. *Microbiol Mol Biol Rev* **61**, 533-616
13. Jensen, P. O., Kolpen, M., Kragh, K. N., and Kuhl, M. (2017) Microenvironmental characteristics and physiology of biofilms in chronic infections of CF patients are strongly affected by the host immune response. *APMIS* **125**, 276-288
14. Borrero-de Acuna, J. M., Timmis, K. N., Jahn, M., and Jahn, D. (2017) Protein complex formation during denitrification by *Pseudomonas aeruginosa*. *Microb Biotechnol* **10**, 1523-1534
15. Stenmark, P., Grunler, J., Mattsson, J., Sindelar, P. J., Nordlund, P., and Berthold, D. A. (2001) A new member of the family of di-iron carboxylate proteins. Coq7 (clk-1), a membrane-bound hydroxylase involved in ubiquinone biosynthesis. *J Biol Chem* **276**, 33297-33300
16. Jiang, H. X., Wang, J., Zhou, L., Jin, Z. J., Cao, X. Q., Liu, H., Chen, H. F., and He, Y. W. (2019) Coenzyme Q biosynthesis in the biopesticide Shenqinmycin-producing *Pseudomonas aeruginosa* strain M18. *J Ind Microbiol Biotechnol*
17. Coelho, C., and Romao, M. J. (2015) Structural and mechanistic insights on nitrate reductases. *Protein Sci* **24**, 1901-1911
18. Hajj Chehade, M., Loiseau, L., Lombard, M., Pecqueur, L., Ismail, A., Smadja, M., Golinelli-Pimpaneau, B., Mellot-Draznieks, C., Hamelin, O., Aussel, L., Kieffer-Jaquinod, S., Labessan, N., Barras, F., Fontecave, M., and Pierrel, F. (2013) *ubiI*, a new gene in *Escherichia coli*

coenzyme Q biosynthesis, is involved in aerobic C5-hydroxylation. *J Biol Chem* **288**, 20085-20092
19. Loiseau, L., Fyfe, C., Aussel, L., Hajj Chehade, M., Hernandez, S. B., Faivre, B., Hamdane, D., Mellot-Draznieks, C., Rascalou, B., Pelosi, L., Velours, C., Cornu, D., Lombard, M., Casadesus, J., Pierrel, F., Fontecave, M., and Barras, F. (2017) The UbiK protein is an accessory factor necessary for bacterial ubiquinone (UQ) biosynthesis and forms a complex with the UQ biogenesis factor UbiJ. *J Biol Chem* **292**, 11937-11950
20. Hille, R. (2005) Molybdenum-containing hydroxylases. *Arch Biochem Biophys* **433**, 107-116
21. Filiatrault, M. J., Picardo, K. F., Ngai, H., Passador, L., and Iglewski, B. H. (2006) Identification of *Pseudomonas aeruginosa* genes involved in virulence and anaerobic growth. *Infect Immun* **74**, 4237-4245
22. Imlay, J. A. (2006) Iron-sulphur clusters and the problem with oxygen. *Mol Microbiol* **59**, 1073-1082
23. Ollagnier de Choudens, S., and Barras, F. (2017) Genetic, Biochemical, and Biophysical Methods for Studying FeS Proteins and Their Assembly. *Methods Enzymol* **595**, 1-32
24. Ollagnier-de Choudens, S., Loiseau, L., Sanakis, Y., Barras, F., and Fontecave, M. (2005) Quinolinate synthetase, an iron-sulfur enzyme in NAD biosynthesis. *FEBS Lett* **579**, 3737-3743
25. Groenewold, M. K., Massmig, M., Hebecker, S., Danne, L., Magnowska, Z., Nimtz, M., Narberhaus, F., Jahn, D., Heinz, D. W., Jansch, L., and Moser, J. (2018) A phosphatidic acid-binding protein is important for lipid homeostasis and adaptation to anaerobic biofilm conditions in *Pseudomonas aeruginosa*. *Biochem J* **475**, 1885-1907
26. Dowhan, W. (1997) Molecular basis for membrane phospholipid diversity: why are there so many lipids? *Annu Rev Biochem* **66**, 199-232
27. Aussel, L., Pierrel, F., Loiseau, L., Lombard, M., Fontecave, M., and Barras, F. (2014) Biosynthesis and physiology of coenzyme Q in bacteria. *Biochim Biophys Acta* **1837**, 1004-1011
28. Sharma, P., Teixeira de Mattos, M. J., Hellingwerf, K. J., and Bekker, M. (2012) On the function of the various quinone species in *Escherichia coli*. *FEBS J* **279**, 3364-3373
29. Nitzschke, A., and Bettenbrock, K. (2018) All three quinone species play distinct roles in ensuring optimal growth under aerobic and fermentative conditions in *E. coli* K12. *PLoS One* **13**, e0194699
30. Filiatrault, M. J., Wagner, V. E., Bushnell, D., Haidaris, C. G., Iglewski, B. H., and Passador, L. (2005) Effect of anaerobiosis and nitrate on gene expression in *Pseudomonas aeruginosa*. *Infect Immun* **73**, 3764-3772
31. Wu, M., Guina, T., Brittnacher, M., Nguyen, H., Eng, J., and Miller, S. I. (2005) The *Pseudomonas aeruginosa* proteome during anaerobic growth. *J Bacteriol* **187**, 8185-8190
32. Worlitzsch, D., Tarran, R., Ulrich, M., Schwab, U., Cekici, A., Meyer, K. C., Birrer, P., Bellon, G., Berger, J., Weiss, T., Botzenhart, K., Yankaskas, J. R., Randell, S., Boucher, R. C., and Doring, G. (2002) Effects of reduced mucus oxygen concentration in airway *Pseudomonas* infections of cystic fibrosis patients. *J Clin Invest* **109**, 317-325
33. Kolpen, M., Hansen, C. R., Bjarnsholt, T., Moser, C., Christensen, L. D., van Gennip, M., Ciofu, O., Mandsberg, L., Kharazmi, A., Doring, G., Givskov, M., Hoiby, N., and Jensen, P. O. (2010) Polymorphonuclear leucocytes consume oxygen in sputum from chronic *Pseudomonas aeruginosa* pneumonia in cystic fibrosis. *Thorax* **65**, 57-62
34. Kolpen, M., Bjarnsholt, T., Moser, C., Hansen, C. R., Rickelt, L. F., Kuhl, M., Hempel, C., Pressler, T., Hoiby, N., and Jensen, P. O. (2014) Nitric oxide production by polymorphonuclear leucocytes in infected cystic fibrosis sputum consumes oxygen. *Clin Exp Immunol* **177**, 310-319
35. Linnane, S. J., Keatings, V. M., Costello, C. M., Moynihan, J. B., O'Connor, C. M., Fitzgerald, M. X., and McLoughlin, P. (1998) Total sputum nitrate plus nitrite is raised during acute pulmonary infection in cystic fibrosis. *Am J Respir Crit Care Med* **158**, 207-212
36. Skurnik, D., Roux, D., Aschard, H., Cattoir, V., Yoder-Himes, D., Lory, S., and Pier, G. B. (2013) A comprehensive analysis of *in vitro* and *in vivo* genetic fitness of *Pseudomonas aeruginosa* using high-throughput sequencing of transposon libraries. *PLoS Pathog* **9**, e1003582

37. Navais, R., Mendez, J., Perez-Pascual, D., Cascales, D., and Guijarro, J. A. (2014) The yrpAB operon of *Yersinia ruckeri* encoding two putative U32 peptidases is involved in virulence and induced under microaerobic conditions. *Virulence* **5**, 619-624
38. Sakai, Y., Kimura, S., and Suzuki, T. (2019) Dual pathways of tRNA hydroxylation ensure efficient translation by expanding decoding capability. *Nat Commun* **10**, 2858
39. Lauhon, C. T. (2019) Identification and Characterization of Genes Required for 5-Hydroxyuridine Synthesis in *Bacillus subtilis* and *Escherichia coli* tRNA. *J Bacteriol* **201**
40. Aussel, L., Loiseau, L., Hajj Chehade, M., Pocachard, B., Fontecave, M., Pierrel, F., and Barras, F. (2014) ubiJ, a new gene required for aerobic growth and proliferation in macrophage, is involved in coenzyme Q biosynthesis in *Escherichia coli* and *Salmonella enterica* serovar *Typhimurium*. *J Bacteriol* **196**, 70-79
41. Held, K., Ramage, E., Jacobs, M., Gallagher, L., and Manoil, C. (2012) Sequence-verified two-allele transposon mutant library for *Pseudomonas aeruginosa* PAO1. *J Bacteriol* **194**, 6387-6389
42. Jacobs, M. A., Alwood, A., Thaipisuttikul, I., Spencer, D., Haugen, E., Ernst, S., Will, O., Kaul, R., Raymond, C., Levy, R., Chun-Rong, L., Guenthner, D., Bovee, D., Olson, M. V., and Manoil, C. (2003) Comprehensive transposon mutant library of *Pseudomonas aeruginosa*. *Proc Natl Acad Sci U S A* **100**, 14339-14344
43. Wagner, V. E., Bushnell, D., Passador, L., Brooks, A. I., and Iglewski, B. H. (2003) Microarray analysis of *Pseudomonas aeruginosa* quorum-sensing regulons: effects of growth phase and environment. *J Bacteriol* **185**, 2080-2095
44. Hassett, D. J. (1996) Anaerobic production of alginate by *Pseudomonas aeruginosa*: alginate restricts diffusion of oxygen. *J Bacteriol* **178**, 7322-7325
45. Jeong, J. Y., Yim, H. S., Ryu, J. Y., Lee, H. S., Lee, J. H., Seen, D. S., and Kang, S. G. (2012) One-step sequence- and ligation-independent cloning as a rapid and versatile cloning method for functional genomics studies. *Appl Environ Microbiol* **78**, 5440-5443
46. Figurski, D. H., and Helinski, D. R. (1979) Replication of an origin-containing derivative of plasmid RK2 dependent on a plasmid function provided in trans. *Proc Natl Acad Sci U S A* **76**, 1648-1652
47. Kavran, J. M., Klein, D. E., Lee, A., Falasca, M., Isakoff, S. J., Skolnik, E. Y., and Lemmon, M. A. (1998) Specificity and promiscuity in phosphoinositide binding by pleckstrin homology domains. *J Biol Chem* **273**, 30497-30508
48. Fish, W. W. (1988) Rapid colorimetric micromethod for the quantitation of complexed iron in biological samples. *Methods in enzymology* **158**, 357-364
49. Beinert, H. (1983) Semi-micro methods for analysis of labile sulfide and of labile sulfide plus sulfane sulfur in unusually stable iron-sulfur proteins. *Analytical biochemistry* **131**, 373-378
50. Rietsch, A., Vallet-Gely, I., Dove, S. L., and Mekalanos, J. J. (2005) ExsE, a secreted regulator of type III secretion genes in *Pseudomonas aeruginosa*. *Proc Natl Acad Sci U S A* **102**, 8006-8011
51. Baynham, P. J., Ramsey, D. M., Gvozdyev, B. V., Cordonnier, E. M., and Wozniak, D. J. (2006) The *Pseudomonas aeruginosa* ribbon-helix-helix DNA-binding protein AlgZ (AmrZ) controls twitching motility and biogenesis of type IV pili. *J Bacteriol* **188**, 132-140

Table 1: Spectral characterization of $UbiV_{Pa}$ and its variants.

Proteins	A_{280}/A_{410}	Content (nmoles/nmole of protein)[1]	
		Iron	Sulfur
$UbiV_{Pa}$ WT	5.8	3.90 ± 0.03	3.40 ± 0.20
$UbiV_{Pa}$ C39AC180A	9.0	1.10 ± 0.16	1.60 ± 0.19
$UbiV_{Pa}$ C193AC197A	7.8	2.90 ± 0.05	3.00 ± 0.12
$UbiV_{Pa}$ C39AC193AC197A	nd	nd	nd

[1]Iron and sulfur quantification of $UbiV_{Pa}$ and its variants. Shown are metal content and UV-vis properties after anaerobic reconstitution of their [Fe-S] clusters for wild-type and variants. nd: not determined.

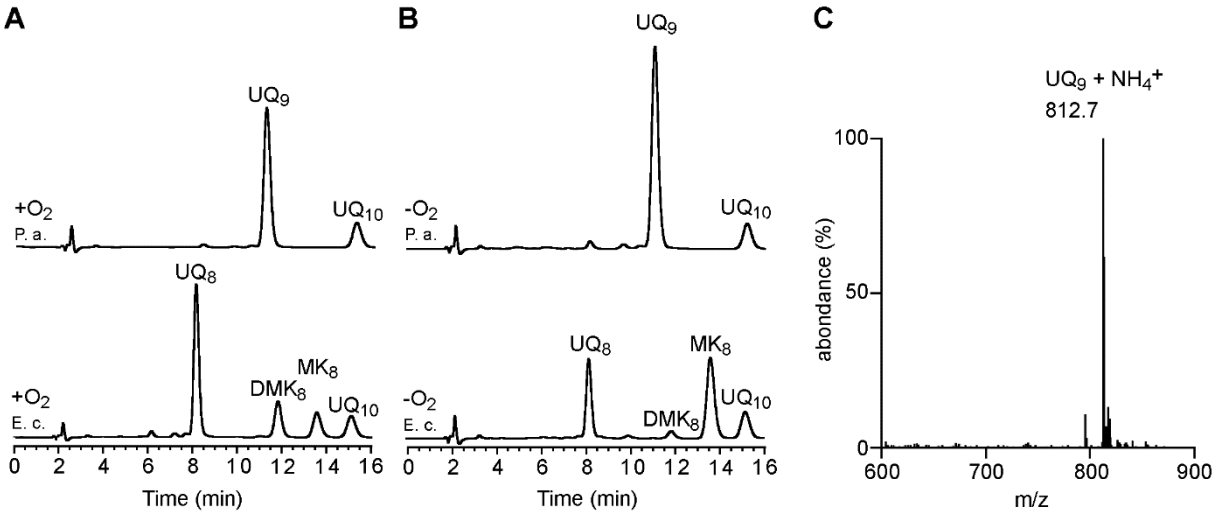


Figure 1: UQ_9 is the major quinone used by *P. aeruginosa* in aerobic and anaerobic conditions. HPLC-ECD analysis of lipid extracts from 1 mg of cells after growth of *E. coli* MG1655 (E. c.) and *P. aeruginosa* PAO1 (P. a.) aerobically ($+O_2$) in LB medium (*A*) or anaerobically ($-O_2$) in denitrification medium (*B*). The chromatograms are representative of three independent experiments. The peaks corresponding to UQ_8, UQ_9, DMK_8, MK_8 and the UQ_{10} as a standard are indicated. *C*, Mass spectrum of the quinone eluting at 11.5 min from extracts of *P. aeruginosa* grown in aerobic and anaerobic cultures.

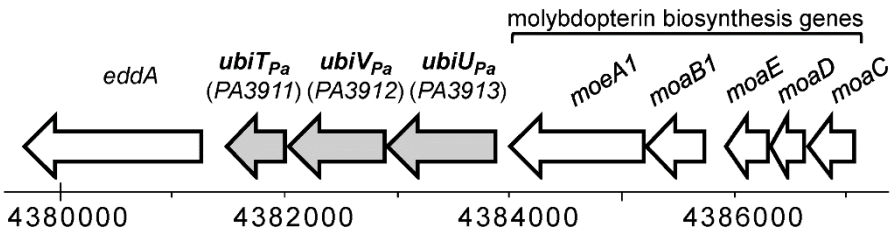


Figure 2: Genomic localization of the *ubiUVT* operon in *P. aeruginosa* PAO1. ORFs of the genes $ubiT_{Pa}$, $ubiU_{Pa}$ and $ubiV_{Pa}$ are represented by grey arrows.

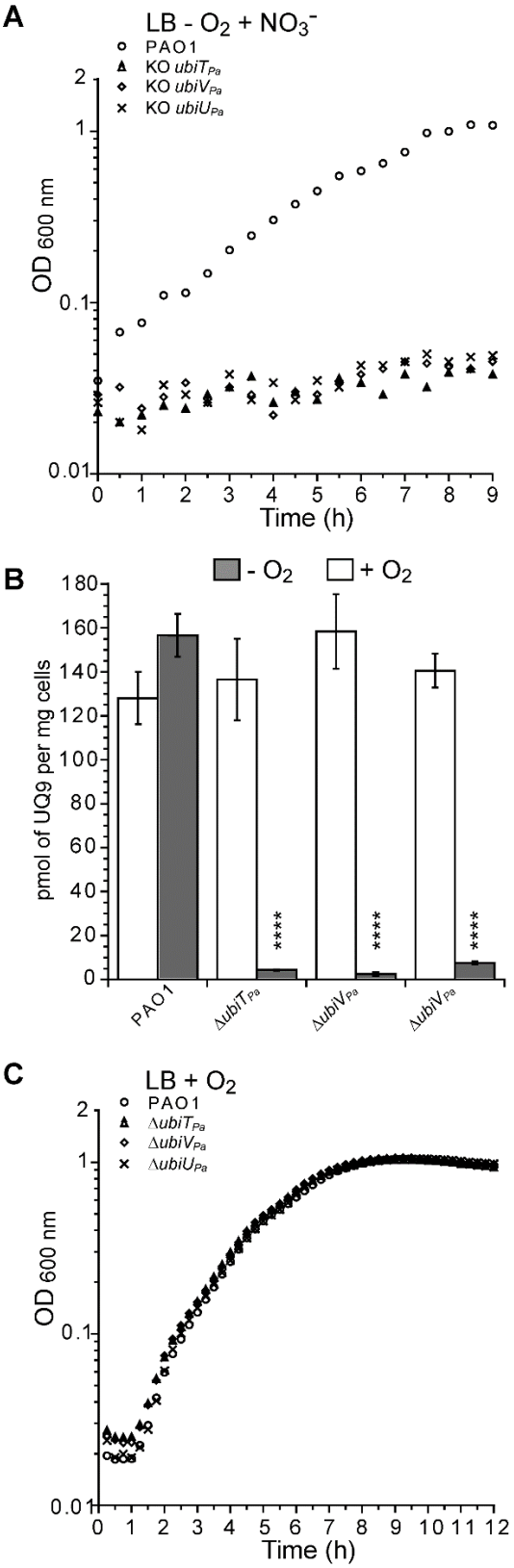


Figure 3: *ubiU*$_{Pa}$, *ubiV*$_{Pa}$ *and ubiT*$_{Pa}$ are essential genes for anaerobic UQ_9 biosynthesis and for denitrification. Representative growth curves of wild-type PAO1 and *ubiTUV*-KO strains grown (*A*) in denitrification medium or (*C*) aerobically in LB medium. *B,* Quantification of cellular UQ_9 content (n=3) in lipid extracts from wild-type PAO1 and KO cells grown aerobically in LB medium (white bars, $P > 0.05$ by unpaired Student's t test) or in denitrification medium (grey bars, ****$P < 0.0001$ by unpaired Student's t test). Error bars represent S.D.

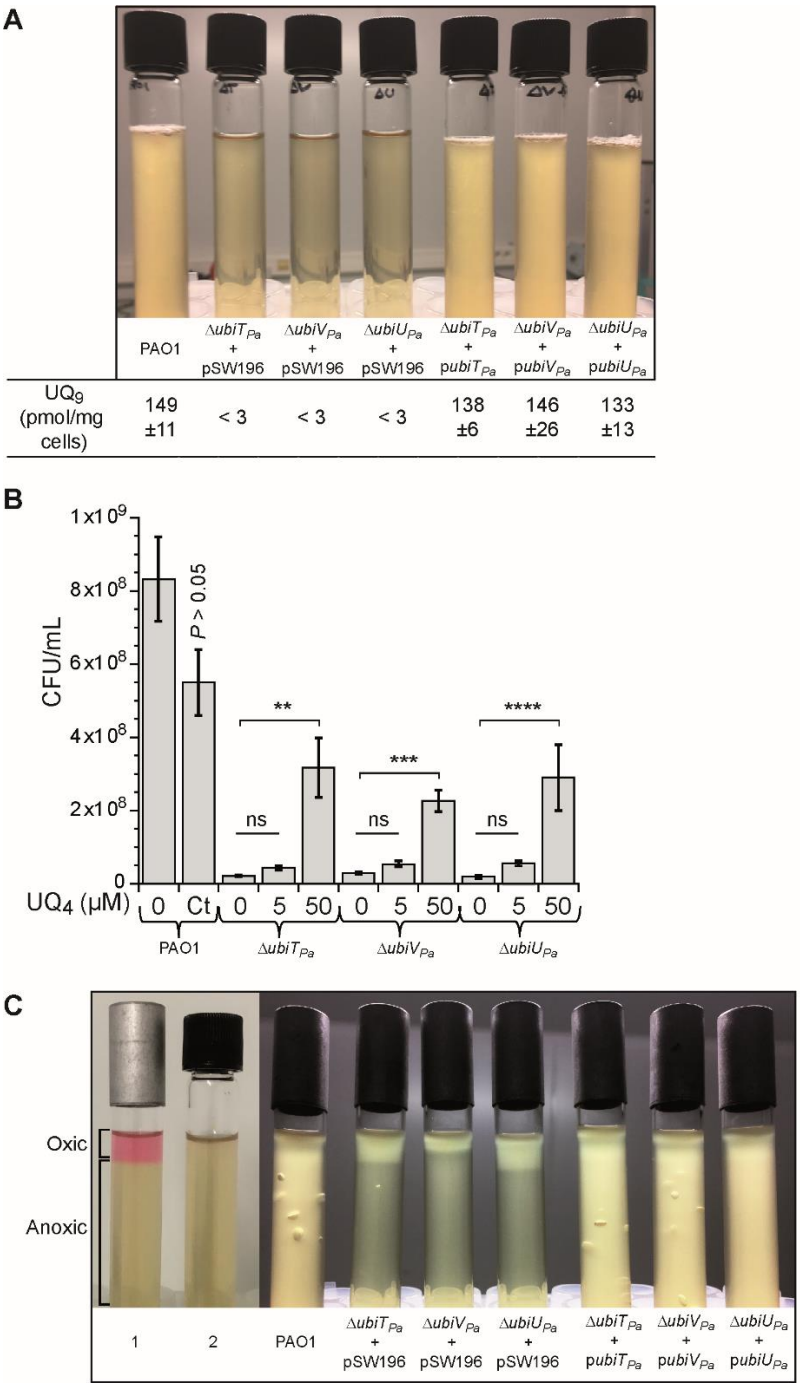


Figure 4: Complementation of *ubiTUV*-KO strains restores bacterial growth over the entire O_2 range in a UQ-dependent manner. *A,* Photographs of culture tubes after overnight growth under anaerobic conditions in denitrification medium of *ubiTUV*-KO strains transformed with the empty vector pSW196 or the same vector carrying the corresponding wild-type allele (*ubiT*$_{Pa}$, *ubiU*$_{Pa}$ and *ubiV*$_{Pa}$). The parental strain PAO1 was used as a control and UQ_9 content of wild-type and *ubiTUV*-KO strains cultured anaerobically was assayed (n=3). *B, ubiTUV*-KO strains were cultured in denitrification medium supplemented with methanol-solubilized UQ_4 at 5 or 50 µM final concentration. After 24h of incubation, colony-forming units per mL (CFU/mL) of each KO strain were estimated and compared to the same strain grown without UQ_4. As a control ($P > 0.05$ by unpaired Student's t test), toxicity of methanol was tested on the parental strain grown in the same medium but supplemented with 4.5% (v/v) methanol (Ct), which is the final concentration of methanol corresponding to the adding of 50 µM of UQ_4. Data are representative of three independent experiments (**$P < 0.01$; ***$P < 0.001$; ****$P < 0.0001$; by

unpaired Student's *t* test compared to condition without addition of UQ_4; ns: no significant). *C,* As in *A,* but in soft-agar tubes after overnight culture. All the strains studied were inoculated into anaerobic tubes and then exposed to ambient air to create an oxygen gradient. The controls (Ct) correspond to soft agar tubes supplemented with 2.5 µg/mL resazurin and then incubated with (1) or without air (2). Oxic and anoxic parts of the agar are indicated. For all strains containing pSW196 vectors, denitrification medium was also supplemented with 0.1% (w/v) final concentration of arabinose to induce P_{BAD} promoter.

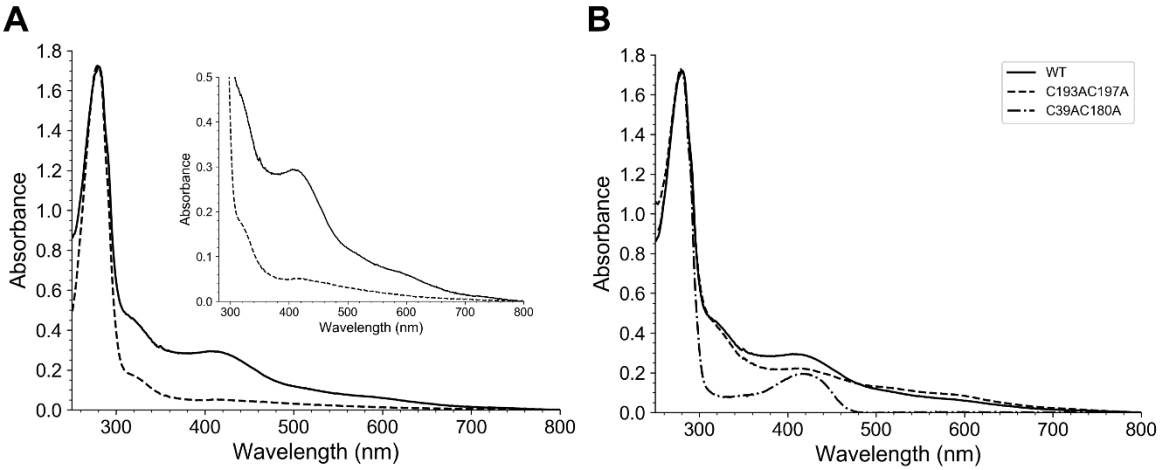


Figure 5: Recombinant $UbiV_{Pa}$ is a [4Fe-4S] cluster-containing protein. *A*, UV-visible absorption of as-purified $UbiV_{Pa}$ (dotted line, 32.6 µM) and reconstituted holo-$UbiV_{Pa}$ (solid line, 22.7 µM). The inset is an enlargement of the 300 to 800 nm region. The molar extinction coefficient, ε_{410nm} was determined to be 12.95 ± 0.5 mM^{-1} cm^{-1} for holo-$UbiV_{Pa}$. *B*, Comparative UV-visible absorption spectra of wild-type and different Cys-to-Ala mutants of $UbiV_{Pa}$ after metal cluster reconstitution. Proteins were analyzed at the following concentrations: 22.7µM WT, 34.8 µM C39AC180A and 15.9 µM C193AC197A. Proteins were suspended in buffer 50 mM Tris-HCl, 25 mM NaCl, 15% (v/v) glycerol, 1 mM DTT, pH 8.5.

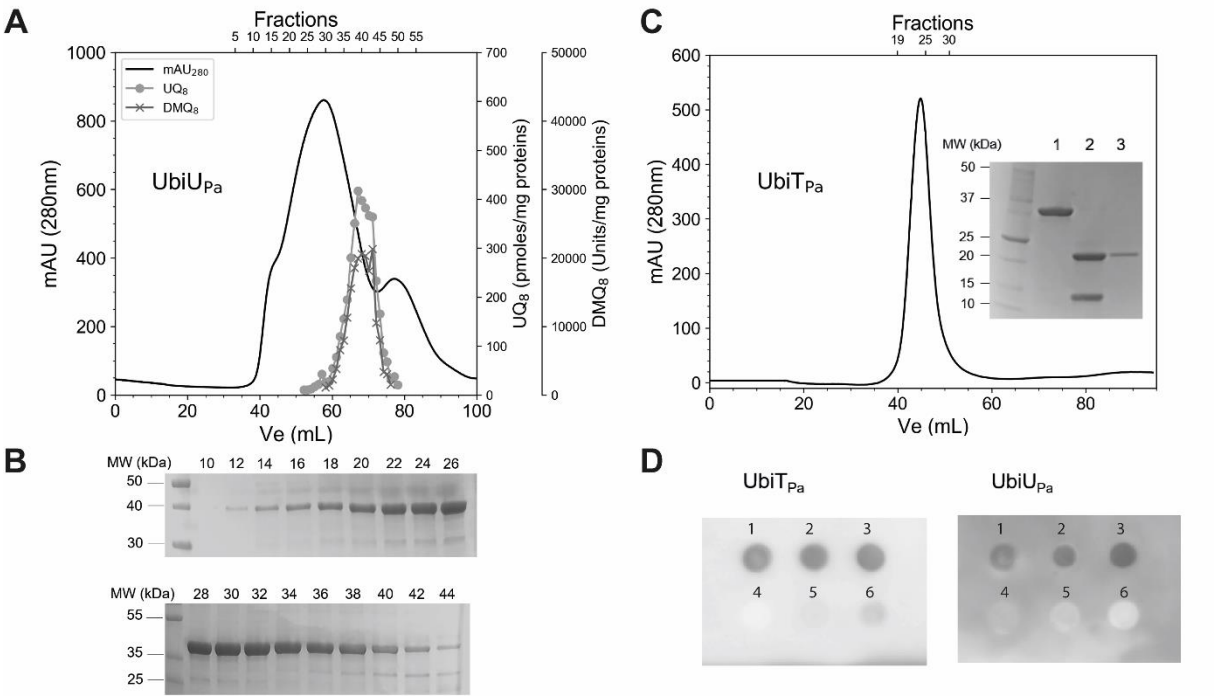


Figure 6: Recombinant $UbiU_{Pa}$ and $UbiT_{Pa}$ bind UQ_8. *A*, Elution profile of $UbiU_{Pa}$, 70 mg of protein were loaded on a Superdex 200 16/60 chromatography column. A quantification of UQ_8 and DMQ_8 in each fraction was performed by HPLC-ECD MS. A recovery of 73 and 76%, respectively for UQ_8 and DMQ_8, was calculated from the total content of all fractions compared with content of the $UbiU_{Pa}$ purified fraction deposited on the Superdex 200 column. *B*, Fractions 10 to 44 analyzed by SDS-PAGE for purity. *C*, Elution profile of $UbiT_{Pa}$ on a Superdex 200 16/60 column. Inset, SDS-PAGE, lane 1, 32 kDa TrxA-$UbiT_{Pa}$ fusion protein, lane 2, after digestion with thrombin ($UbiT_{Pa}$, 19.6kDa and TrxA, 12.1 kDa), lane 3, pooled fractions 20-30 of $UbiT_{Pa}$. Quantification of UQ_8 (pool of fractions 20 to 30) was performed by HPLC-ECD MS. *D*, Protein-lipid overlay assay between $UbiU_{Pa}$ and $UbiT_{Pa}$ and different lipid ligands. 2 µL of six different lipid/compound potential candidates (1, UQ_8; 2, UQ_{10}; 3, solanesol; 4, 3-methylcatechol; 5, cholesterol; 6, POPE) at 20 mM final concentration were spotted on a PVDF membrane and then incubated with $UbiT_{Pa}$ or $UbiU_{Pa}$ (both proteins at 0.2 µg/mL final concentration). Detection of bound proteins was performed by chemiluminescence, as described in Experimental Procedures section. Mw: molecular weights.